The 2025 World Congress on
Advances in Structural Engineering and Mechanics (ASEM25)
BEXCO, Busan, Korea, August 11-14, 2025

Effects of elevated temperature on the tensile behavior of ultra-high performance concrete

Wen-Cheng Yeh[1)], Yuan-Jung Hsu[2)], *Ming-Hui Lee[3)]

[1), 2), 3)] *Department of Civil Engineering, NPUST, Pingtung 912301, Taiwan, Republic of China*
[2)] *Department of Civil Engineering, R.O.C.M.A , Kaohsiung 83055, Taiwan, Republic of China*
[3)] *MHLee61@mail.npust.edu.tw*

ABSTRACT

Ultra-high performance concrete (UHPC) exhibits superior material properties compared to conventional concrete. Its high density, combined with the incorporation of steel fibers, enhances its strength, ductility, and durability, making it a suitable construction material for critical infrastructure. However, the stress behavior of UHPC significantly influences numerical simulation results. When exposed to high temperatures, its stress-strain response affects the accuracy of these simulations. In this study, UHPC dog-bone specimens with a 2% steel fiber volume ratio were tested. The heating process was conducted under two conditions: an ASTM E-119 fire hazard environment and a progressive high-temperature environment. The effects of these thermal conditions on the energy absorption, tensile strength, and strain-hardening behavior of UHPC reinforced with steel fibers were analyzed. Additionally, the fire resistance of UHPC was evaluated by comparing its strength loss under different heating conditions. The findings provide a basis for numerical simulation of UHPC after high-temperature exposure and offer insights for optimizing fire protection measures.

1. INTRODUCTION

The growing demands for enhanced performance and durability in modern concrete structures have catalyzed the advancement of ultra-high performance concrete (UHPC). As an innovative fibre-reinforced cementitious composite, UHPC is distinguished by its exceptional mechanical strength, durability, and ductility (Sharma 2022; Gong 2022; Li 2020; Dong 2025). In comparison to conventional concrete, UHPC enables more compact structural designs, reduced reinforcement needs, improved

---

[1)] Associate Professor

[2)] Graduate Student / Lecturer

[3)] Professor

impact resistance, and superior crack control capabilities (Wang 2025; Abbas 2016; Hung 2021). These outstanding properties make UHPC a highly suitable material for a broad spectrum of structural applications.

An increasing number of researchers are investigating the mechanical behaviour of UHPC under extreme environmental conditions. Owing to its outstanding strength and durability, UHPC has emerged as a preferred material for critical infrastructure, including bridges, airport runways, and high-rise buildings. When subjected to extreme events such as fire or explosions, it is imperative that these structures retain their structural integrity. Consequently, enhancing the fire resistance of UHPC has become a topic of growing significance.

Despite the superior performance of UHPC, it remains susceptible to spalling when exposed to elevated temperatures (Malik 2021; Banerji 2020). Shen (2022) reported that UHPC exhibited a tendency to spall at high temperatures, with an average onset temperature of approximately 588 °C. This phenomenon is primarily attributed to the buildup of internal pore pressure; when this pressure surpasses the material's tensile strength, cracking occurs, ultimately leading to spalling (Du 2020; Figueiredo 2019).

In high-temperature environments, the differential thermal strains between cement paste and aggregates play a critical role in influencing the behaviour of concrete. Owing to the mismatch in thermal expansion coefficients among constituent materials, non-uniform expansion and contraction can induce internal micro-cracking. As ambient temperatures rise, aggregates tend to expand while the cement matrix may contract, further intensifying internal stress imbalances.

One key factor contributing to concrete spalling under elevated temperatures is the moisture retention effect (Fu 2011). When moisture is present, heating causes internal water to vaporize and migrate. While some vapour escapes through the surface, a portion penetrates inward, increasing pore saturation and potentially forming a dense, impermeable layer. Once the internal vapour pressure exceeds the local tensile strength of the concrete, cracking and spalling occur.

Another contributing mechanism is the thermal gradient effect. Rapid temperature increases generate steep internal temperature differentials, leading to significant thermal stresses. If these stresses exceed the material's ultimate strength, they can result in surface delamination and spalling (Liu 2018; Missemer 2019).

To mitigate high-temperature-induced cracking in UHPC, the incorporation of synthetic and steel fiber has been widely adopted as an effective formulation strategy (Sciarretta 2021; Lin 2024; Liu 2021; Li 2018). Several studies have demonstrated that synthetic fibres can significantly enhance the thermal resistance of concrete (Lin 2024; Zhang 2021). When heated to approximately 165 ˚C, synthetic fibres melt and form micro-channels within the matrix, which improve permeability, facilitate the release of internal pore pressure, and alleviate thermal stress gradients (Yang 2019).

In parallel, UHPC is known to release considerable energy during crack propagation; thus, the inclusion of steel fibers serves to enhance its tensile strength and energy absorption capacity. This reinforcement effect further reduces the risk of cracking and spalling under elevated temperatures (Park 2019).

Although numerous studies have explored the behaviour of UHPC reinforced with steel and synthetic fibres under high-temperature conditions, the incorporation of synthetic fibres has been shown to reduce both compressive strength and tensile

performance (Lin 2024; Gong 2022). Moreover, research specifically examining the tensile behaviour and residual stress characteristics of UHPC reinforced solely with steel fibers at elevated temperatures remains limited. The majority of existing studies have primarily focused on compressive strength evaluations (Hernández 2024; Abadel 2021), with relatively few addressing tensile properties. In addition, when exposed to temperatures around 400 °C, UHPC specimens often exhibit severe cracking, thereby hindering further investigation into their performance at higher temperatures.

To improve the cracking behaviour of UHPC, two heating curves were employed in this study: the ASTM E-119 standard fire damage curve and a gradual heating curve. In addition to simulating the effects of real fire damage on UHPC, a progressive heating curve was also used for heating. After heating, tensile strength was tested using a direct tensile test. The residual tensile stress of UHPC after exposure to high temperatures was investigated.

2. MATERIAL PROPORTIONS AND EXPERIMENTAL DESIGN

2.1 Material composition ratio

The UHPC specimens used in this study were prepared using the material composition detailed in Table 1. The primary constituents included Type I Portland cement, silica fume, silica powder, silica sand, and water. Given the predominance of fine powdered materials, the resulting UHPC exhibits exceptionally high density. Notably, 50% of the cement was replaced with silica powder, effectively lowering the water-to-cement ratio. This substitution also contributes to reduced porosity and enhanced interfacial properties within the UHPC matrix. Furthermore, a superplasticizer was incorporated to maintain adequate workability while minimizing water demand.

Table 1 Main constituents of UHPC

Portland Type I cement	Silica fume	Silica Powder	Silica sand	Water	Superplasticizer	Steel fiber*
0.5	0.5	0.25	0.462	0.19	0.015	2.0%

* The amount of steel fiber is the volume ratio of the mixture

To investigate the effects of steel fibers on the performance of UHPC under varying temperature conditions, straight steel fibers were incorporated at a volume fraction of 2%. The mechanical properties of the fibres are presented in Table 2.

Table 2 Properties of the steel fibers

Fiber Shape	Length (mm)	Diameter (mm)	Aspect ratio (l_{sf}/d_{sf})	Tensile Strength (MPa)
Straight smooth	13	0.2	65	>2800

2.2 Specimen preparation and curing process

In this study, twelve cube specimens (50 mm × 50 mm × 50 mm) and seven dog-bone specimens were cast. Compressive strength tests were conducted at 3, 7, and 28 days, followed by direct tensile tests on the dog-bone specimens.

During the preparation of UHPC, dry materials—including cementitious powders and quartz sand—were first mixed at low speed for 5 minutes to prevent clumping and ensure uniform distribution. Separately, water and a superplasticizer were thoroughly blended and gradually added to the dry mix while stirring continued. After approximately 5 minutes, the mixture began to react; mixing was then continued for an additional 8 minutes until a homogeneous paste with adequate flowability was achieved.

steel fibers were subsequently incorporated and mixed for another 5 minutes to ensure uniform dispersion within the matrix. Prior to casting, a fluidity test was performed to verify workability. The fresh UHPC paste was then poured into moulds and covered with plastic wrap to minimize drying shrinkage. After 24 hours, the specimens were demoulded and subjected to heat curing at 90 °C for 72 hours in a constant-temperature curing chamber. Following thermal curing, the specimens were stored at ambient conditions and allowed to age for 28 days before testing.

2.3 Experimental methodology

2.3.1 Fluidity test and compressive test

The fundamental performance evaluations in this study included a fluidity test and a compressive test. The fluidity test was conducted in accordance with ASTM C1437-20 (2020). After placing the fresh UHPC paste into a standard conical mould without compaction, the mould was carefully lifted to allow the paste to spread freely. The spread diameter was measured along both the horizontal and vertical directions within 2 minutes, and the average of the two measurements was recorded as the final flow value.

The compressive test was conducted in accordance with ASTM C109 (2016). Tests were performed on cube specimens at curing ages of 3, 7, and 28 days using a fully automated compression testing machine, as illustrated in Fig. 1. For each age group, three specimens were tested, and the average compressive strength along with the standard deviation was calculated.

Fig. 1 SUMMIT KH-2000 compressive tester

2.3.2 Heating type

All test specimens were aged for 28 days prior to high-temperature exposure. To mitigate the risk of explosive spalling during heating, the specimens were oven-dried at 90 °C for 7 days. Subsequent heating tests were conducted using a high-temperature furnace equipped with an automatic temperature controller. The furnace had internal dimensions of 150 mm (W) × 100 mm (H) × 300 mm (D) and a maximum operating temperature of 1000 °C. The heating rate was set at 30 °C/min, as shown in Fig. 2.

Fig. 2 Heating furnace

This test employs two heating types, as shown in Fig. 3. The first method follows the standard heating curve listed in ASTM E-119 to raise the temperature. The second method uses a gradual heating curve with a uniform heating rate of 1 °C/min to reach the set temperature. Once the test specimen reaches the set temperature, it is held at that temperature for 30 minutes to ensure thermal stability. Both methods target test temperatures of 100 °C, 200 °C, and 300 °C. The specimens are allowed to cool naturally to room temperature inside the high-temperature furnace before undergoing direct tensile performance testing.

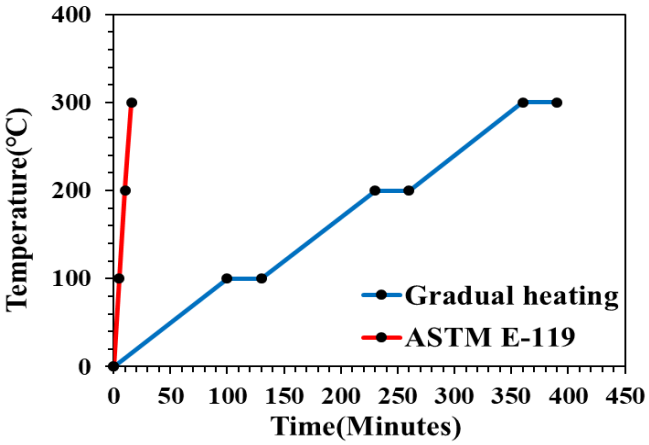

Fig. 3 Heating curve

2.3.3 Tensile performance test

Direct tensile strength tests were conducted using an MTS 819 servo-hydraulic testing machine, with a controlled tensile strain rate of 0.001 mm/s. For each mixture type, two dog-bone specimens were tested at target temperatures of 100 °C, 200 °C, and 300 °C under different heating protocols, as illustrated in Fig. 4(a). The average values were used to construct the corresponding tensile stress–strain curves.

Axial force was measured using a Kistler 9351B piezoelectric force transducer, while specimen elongation was recorded via linear variable differential transformers (LVDT) mounted on both sides of the specimen. The LVDTs were secured below the specimen with clamps, while upper clamps served as boundary constraints. A schematic diagram of the direct tensile testing setup is provided in Fig. 4(b).

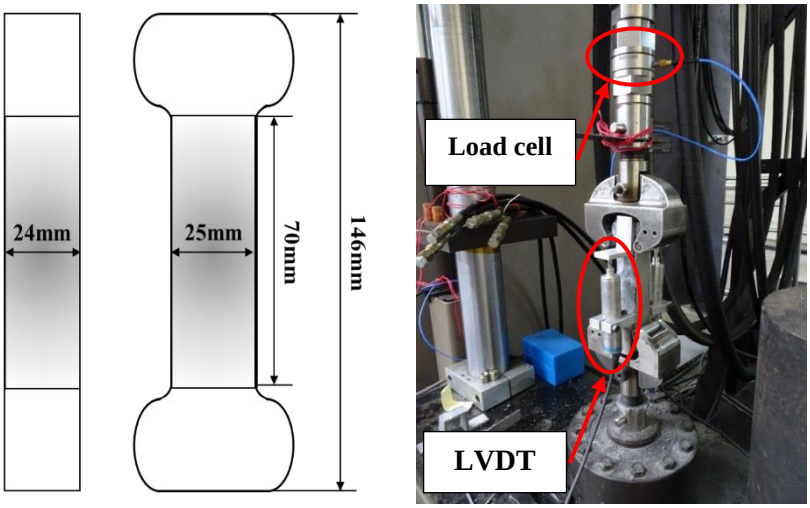

(a)Dog bone specimen (b)Test setup

Fig. 4 Direct tensile test

3. ANALYSIS OF TEST RESULTS

3.1 Material basic performance analysis

The average flowability of the UHPC mixtures was measured at 248 mm, indicating excellent workability. The compressive strengths at different curing ages are presented in Fig. 5. At 28 days, the compressive strength reached 150 MPa, with a consistent increase observed across all age groups. The early strength gain is attributed to enhanced interfacial bonding between the matrix and steel fibers, facilitated by thermal curing. Furthermore, accelerated hydration during heat curing reduces the risk of micro-crack formation associated with shrinkage stress.

In the mix design, 50% of the cement was replaced with silica fume. During the later stages of curing, the slag powder reacts with calcium hydroxide-a byproduct of cement hydration-to form additional calcium silicate hydrate (C-S-H), contributing to a denser microstructure and improved mechanical strength.

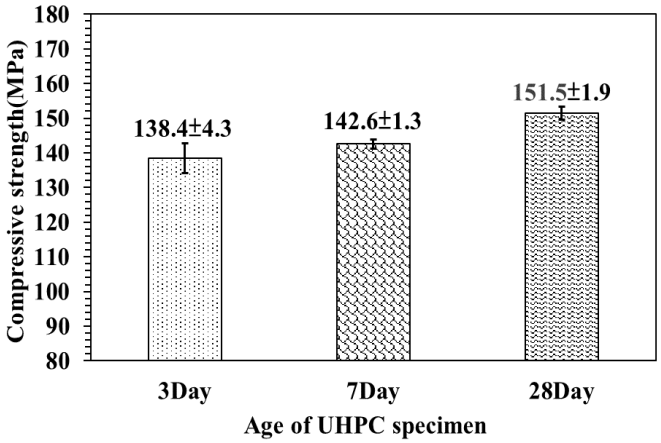

Fig. 5 Compressive strength

3.2 Stress-strain behavior

The direct tensile stress-strain curves of UHPC containing 2% steel fibers under different heating types are presented in Fig. 6. The tensile stress-strain behaviour at 300°C for both heating types is identical to that of the traditional tensile curve. Following the initial elastic stage, the stress-strain curves exhibit a distinct cracking point, after which the material undergoes strain hardening. Upon the formation of primary cracks, the response transitions into the strain-softening stage.

Hung (2024) reported an increase in tensile strength of UHPC when exposed to temperatures of 100 °C and 200 °C. This enhancement was attributed to continued hydration reactions, which increase the formation of calcium silicate hydrate (C-S-H) gel and calcium hydroxide (C-H), thereby improving matrix strength and enhancing the interfacial bond between steel fibers and the matrix. Additionally, moisture loss during the drying process reduces pore water pressure and contributes to stronger interfacial bonding, further supporting the observed strength gain.

However, this phenomenon was not observed in the present study. The primary reason is that the specimens were pre-dried in a 90 °C oven for 7 days prior to testing, resulting in substantial moisture loss from the interior. As a result, no additional strength

gain was detected at 100 °C or 200 °C; instead, a decline in tensile strength was observed. At 300 °C, the reduction in strength became more pronounced. These trends are reflected in the tensile stress-strain curves obtained under the two heating types, as shown in Fig. 6(a) and 6(b).

Although strength decreases under both heating types, the tensile stress–strain curve profiles exhibit slight differences at the same target temperature. As shown in Fig. 6(a) and 6(b), the strain corresponding to the peak stress increases with rising temperature, indicating enhanced ductility at elevated temperatures. This suggests that while the tensile strength of UHPC diminishes under high-temperature exposure, its deformation capacity prior to failure improves. This effect is particularly evident in Fig. 6(b).

At 300 °C, steel fibers largely retain their mechanical properties and continue to provide a bridging effect after the initiation of cracking. However, prolonged exposure to high temperatures reduces the bond strength and interfacial friction between the steel fibers and the cementitious matrix, leading to fibre pull-out rather than rupture. This mechanism contributes to the more ductile response observed in the stress–strain curves.

Under the gradual heating regime, the strain-hardening behaviour becomes more pronounced, and in the subsequent strain-softening stage, the decline in stress is less abrupt. This moderated softening may be attributed to microstructural degradation of the UHPC matrix caused by the extended duration of thermal exposure.

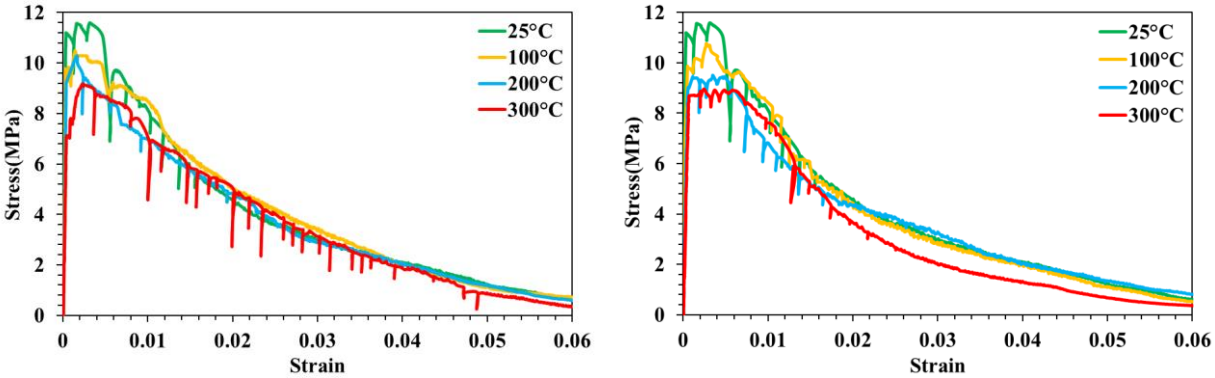

(a)ASTM E-119 (b)Gradual heating

Fig. 6 Tensile test results of UHPC after exposure to different heating types

3.3 Analysis of tensile properties parameters

To evaluate the tensile behaviour of UHPC under different heating types, several key parameters were defined and analysed in this study. The initial cracking strength, denoted as σ_{cc}, corresponds to the stress at the inflection point where the material transitions from the elastic stage to the strain-hardening stage (point A in Fig. 7). The ultimate cracking strength, σ_{pc}, refers to the maximum tensile stress observed after initial cracking, located at the peak of the curve (point B). Point C represents the point at which the tensile stress drops to zero.

The corresponding strain values are denoted as ε_{cc} for the initial cracking strength and ε_{pc} for the ultimate cracking strength. The absorbed energy, g, is defined as the area under the stress–strain curve from the origin (point O) to the peak stress (point B),

reflecting the energy absorbed by the specimen before the onset of softening. Following peak stress, the formation of primary cracks and the bridging action of steel fibers lead to strain-softening behaviour.

The fracture energy, G_f, is defined as the area under the curve from the peak (point B) to the point of zero stress (point C), representing the energy dissipated during the post-peak fracture process. In this study, all energy-related parameters were calculated up to a maximum strain of 0.06 to ensure consistency across specimens.

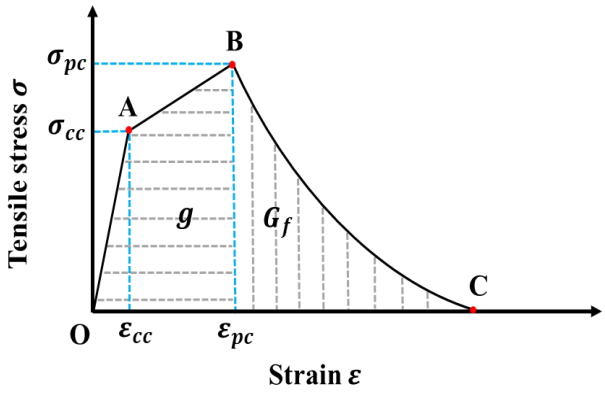

Fig. 7 Sketch of the stress-strain curve of direct tensile test (Wang 2023)

The results of the key tensile parameters are summarized in Table 3, providing a comprehensive dataset for evaluating the effects of high-temperature exposure and different heating types on the tensile performance of UHPC. Under ambient conditions (25 °C), the ultimate tensile strength (σ_{pc}), absorbed energy (g), and fracture energy (G_f) demonstrate stable tensile behaviour. These results indicate that UHPC exhibits high toughness and effective crack control capacity in the unheated state.

Table 3 Test results

Heating type	Temperature	σ_{cc}	ε_{cc}	σ_{pc}	ε_{pc}	g	G_f
-	℃	MPa	mm/mm	MPa	mm/mm	kJ/m^3	kJ/m^3
Room temperature	25	11.19	0.00036	11.56	0.00159	15.93	230.62
ASTM E-119	100	9.77	0.00028	10.49	0.00143	12.22	237.29
	200	9.22	0.00037	10.25	0.00156	13.28	214.59
	300	8.17	0.00044	9.18	0.00237	17.38	207.54
Gradual heating	100	9.85	0.00052	10.76	0.00275	25.45	210.53
	200	9.01	0.00068	9.51	0.00352	29.79	198.51
	300	8.67	0.00071	8.91	0.00492	40.01	155.12

Under the heating conditions specified by ASTM E119, the mechanical properties of UHPC degrade progressively with increasing temperature. While Hung et al. [30] reported an increase in tensile strength at 100 °C and 200 °C-attributed to drying and hardening, hydrothermal phase transformations, moisture-induced internal pressure, and

continued hydration-such improvements were not observed in the present study, as indicated by the parameter values in Table 3. Specifically, the ultimate tensile strength (σ_{pc}) decreased by 10.2%, 11.3%, and 20.6% at 100 °C, 200 °C, and 300 °C, respectively, compared to the unheated specimens.

This discrepancy is primarily due to the pre-drying treatment applied in this study, wherein specimens were oven-dried at 90 °C for 7 days, resulting in significant moisture loss and thereby limiting further hydration during subsequent heating. Additionally, the strain corresponding to σ_{pc} increased with temperature, indicating enhanced deformability at elevated temperatures and a corresponding rise in absorbed energy (g).

As for the fracture energy (G_f), values at 100 °C were comparable to those at ambient temperature. However, at 200 °C and 300 °C, G_f declined by 6.9% and 10.0%, respectively, suggesting a gradual reduction in the crack-bridging and energy dissipation capacity of UHPC during the strain-softening stage.

In comparison, the gradual heating type exerts a more pronounced influence on the strain-hardening behaviour of UHPC. At 100 °C, the ultimate tensile strength (σ_{pc}) is comparable to that obtained under the ASTM E119 standard heating protocol. However, the corresponding strain (ε_{pc}) increases by 92.3%, indicating a substantial enhancement in ductility. This trend becomes more prominent with increasing temperature, reaching its maximum at 300 °C, where ε_{pc} attains the highest value among all tested specimens. These results suggest that gradual heating effectively mitigates thermal stress gradients within UHPC and delays the onset of crack propagation.

Despite the significant increase in deformability, as reflected in the stress–strain curves, the absorbed energy (g) rises by 151.1% relative to the unheated condition (25 °C). However, the fracture energy (G_f) drops to its lowest value, measured at 155.12 kJ/m³. This implies that while gradual heating enhances the material's capacity to absorb energy prior to peak stress, prolonged high-temperature exposure may compromise the post-peak toughness, resulting in a more brittle failure mode.

4. CONCLUSIONS AND RECOMMENDATIONS

This study used two different heating types to heat UHPC with a steel fiber volume ratio of 2% and investigated its direct tensile mechanical properties. The conclusions are as follows:

(1) Between 100°C and 300°C, the tensile strength of UHPC exhibited a decreasing trend compared to that at 25°C. However, some studies have reported strength enhancement under similar conditions. This discrepancy is likely due to residual moisture in the material, which can sustain ongoing hydration reactions at elevated temperatures. In the present study, specimens were preconditioned in a 90°C oven for seven days to eliminate most of the internal moisture, thereby preventing such effects. Consequently, earlier findings may not fully represent the intrinsic thermal response of UHPC. The results of this study offer a more accurate evaluation of the material's performance and its suitability under thermal exposure.

(2) Gradual heating enhances the deformation capacity of UHPC. Compared to the ASTM E-119 standard heating type, the peak strain observed under gradual heating is significantly higher, particularly at 300°C. This indicates that gradual heating

effectively promotes strain hardening behavior, contributing to improved toughness and crack control performance. However, this benefit comes at the expense of reduced tensile strength.

(3) Under high-temperature conditions, both the gradual heating type and the ASTM E-119 standard heating type led to an increase in the absorption energy g; however, the fracture energy G_f decreased. This suggests that more energy is dissipated prior to the formation of the main crack, while the post-cracking softening progresses at a faster rate. These results indicate a qualitative shift in the crack control mechanism at elevated temperatures, with the gradual heating type exhibiting the most pronounced effect. Accordingly, the influence of thermal exposure duration and heating rate must be carefully considered in the assessment of structural safety.

(4) This study examined only a single type of steel fiber. It is recommended that future research incorporate various fiber types, volume fractions, and other influencing parameters to provide a more comprehensive understanding. Such investigations would offer valuable reference data on the tensile behavior of UHPC with different material configurations under high-temperature conditions.

REFERENCES

Sharma, R., Jang, J. G., & Bansal, P. P. (2022). A comprehensive review on effects of mineral admixtures and fibers on engineering properties of ultra-high-performance concrete. Journal of Building Engineering, 45, 103314.

Gong, J., Ma, Y., Fu, J., Hu, J., Ouyang, X., Zhang, Z., & Wang, H. (2022). Utilization of fibers in ultra-high performance concrete: A review. Composites Part B: Engineering, 241, 109995.

Li, P. P., Sluijsmans, M. J., Brouwers, H. J. H., & Yu, Q. L. (2020). Functionally graded ultra-high performance cementitious composite with enhanced impact properties. Composites Part B: Engineering, 183, 107680.

Dong, S., Gu, J., Ouyang, X., Jang, S. H., & Han, B. (2025). Enhancing mechanical properties, durability and multifunctionality of concrete structures via using ultra-high performance concrete layer: A review. Composites Part B: Engineering, 112329.

Wang, Q., Li, Q., Yin, X., & Xu, S. (2025). Micromechanics-informed cohesive fracture analysis of UHPC with emphasis on the combined effect of structural size and fiber content. Engineering Fracture Mechanics, 315, 110810.

Abbas, S. M. L. N., Nehdi, M. L., & Saleem, M. A. (2016). Ultra-high performance concrete: Mechanical performance, durability, sustainability and implementation challenges. International Journal of Concrete Structures and Materials, 10, 271-295.

Hung, C. C., & Yen, C. H. (2021). Compressive behavior and strength model of reinforced UHPC short columns. Journal of Building Engineering, 35, 102103.

Malik, M., Bhattacharyya, S. K., & Barai, S. V. (2021). Thermal and mechanical properties of concrete and its constituents at elevated temperatures: A review. Construction and Building Materials, 270, 121398.

Banerji, S., Kodur, V., & Solhmirzaei, R. (2020). Experimental behavior of ultra high performance fiber reinforced concrete beams under fire conditions. Engineering Structures, 208, 110316.

Shen, Y., Dai, M., Pu, W., & Xiang, Z. (2022). Effects of content and length/diameter ratio of PP fiber on explosive spalling resistance of hybrid fiber-reinforced ultra-high-performance concrete. Journal of Building Engineering, 58, 105071.

Du, Y., Qi, H. H., Huang, S. S., & Liew, J. R. (2020). Experimental study on the spalling behaviour of ultra-high strength concrete in fire. Construction and Building Materials, 258, 120334.

Figueiredo, F. P., Huang, S. S., Angelakopoulos, H., Pilakoutas, K., & Burgess, I. (2019). Effects of recycled steel and polymer fibres on explosive fire spalling of concrete. Fire Technology, 55, 1495-1516.

Fu, Y., & Li, L. (2011). Study on mechanism of thermal spalling in concrete exposed to elevated temperatures. Materials and structures, 44, 361-376.

Liu, J. C., Tan, K. H., & Yao, Y. (2018). A new perspective on nature of fire-induced spalling in concrete. Construction and Building Materials, 184, 581-590.

Missemer, L., Ouedraogo, E., Malecot, Y., Clergue, C., & Rogat, D. (2019). Fire spalling of ultra-high performance concrete: From a global analysis to microstructure investigations. Cement and Concrete Research, 115, 207-219.

Sciarretta, F., Fava, S., Francini, M., Ponticelli, L., Caciolai, M., Briseghella, B., & Nuti, C. (2021). Ultra-High performance concrete (UHPC) with polypropylene (Pp) and steel Fibres: Investigation on the high temperature behaviour. Construction and Building Materials, 304, 124608.

Lin, J., Zhang, Y., Huang, S., Du, H., & Jiang, K. (2024). Influence of synthetic fibers on the performance of ultra-high performance concrete (UHPC) at elevated temperatures. Journal of Building Engineering, 97, 110735.

Liu, J. C., Huang, L., Tian, Z., & Ye, H. (2021). Knowledge-enhanced data-driven models for quantifying the effectiveness of PP fibers in spalling prevention of ultra-high performance concrete. Construction and Building Materials, 299, 123946.

Li, Y., Tan, K. H., & Yang, E. H. (2018). Influence of aggregate size and inclusion of polypropylene and steel fibers on the hot permeability of ultra-high performance concrete (UHPC) at elevated temperature. Construction and Building Materials, 169, 629-637.

Lin, J., Zhang, Y., Guo, Z., & Du, H. (2024). Impact of synthetic fibers on spalling and intrinsic pore structure of ultra-high performance concrete (UHPC) under elevated temperatures. Construction and Building Materials, 439, 137325.

Zhang, D., Zhang, Y., Dasari, A., Tan, K. H., & Weng, Y. (2021). Effect of spatial distribution of polymer fibers on preventing spalling of UHPC at high temperatures. Cement and Concrete Research, 140, 106281.

Yang, J., Peng, G. F., Zhao, J., & Shui, G. S. (2019). On the explosive spalling behavior of ultra-high performance concrete with and without coarse aggregate exposed to high temperature. Construction and Building Materials, 226, 932-944.

Park, J. J., Yoo, D. Y., Kim, S., & Kim, S. W. (2019). Benefits of synthetic fibers on the residual mechanical performance of UHPFRC after exposure to ISO standard fire. Cement and Concrete Composites, 104, 103401.

Lin, J. X., Luo, R. H., Su, J. Y., Guo, Y. C., & Chen, W. S. (2024). Coarse synthetic fibers (PP and POM) as a replacement to steel fibers in UHPC: Tensile behavior, environmental and economic assessment. Construction and Building Materials, 412, 134654.

Gong, J., Ma, Y., Fu, J., Hu, J., Ouyang, X., Zhang, Z., & Wang, H. (2022). Utilization of fibers in ultra-high performance concrete: A review. Composites Part B: Engineering, 241, 109995.

Hernández-Figueirido, D., Reig, L., Melchor-Eixea, A., Roig-Flores, M., Albero, V., Piquer, A., & Pitarch, A. M. (2024). Spalling phenomenon and fire resistance of ultrahigh-performance concrete. Construction and Building Materials, 443, 137695.

Abadel, A. A., & Alharbi, Y. R. (2021). Confinement effectiveness of CFRP strengthened ultra-high performance concrete cylinders exposed to elevated temperatures. Mater. Sci, 39, 478-490.

ASTM C1437-20 [2020] “Standard Test Method for Flow of Hydraulic Cement Mortar,” ASTM International,West Conshohocken, PA.

ASTM C109/C109M-16a [2016] “Standard Test Method for Compressive Strength of Hydraulic Cement Mortars (Using 2-in. or [50-mm] Cube Specimens),” ASTM International, West Conshohocken, PA.

Hung, C. C., Yulianti, E., & Agrawal, S. (2024). Microstructures, durability, and mechanical behavior of hybrid steel and PP fiber reinforced UHPC at elevated temperatures. Construction and Building Materials, 447, 138208.

Wang, S., Xu, L., Yin, C., Cui, K., & Chi, Y. (2023). Constitutive behavior of ultra-high-performance steel fiber reinforced concrete under monotonic and cyclic tension. Journal of Building Engineering, 68, 105991.